Electronic Supporting Information

Factors underlying efficiency of aromatic oxalates in peroxyoxalate chemiluminescent in aqueous-organic media at deficiency of hydrogen peroxide

Evgenii O. Fomin,[a] Nikolai P. Iakimov,[a] Ekaterina M. Budynina,[a,b] Irina D. Grozdova,[a] Nikolay S. Melik-Nubarov [a*]

a) Department of Chemistry, M. V. Lomonosov Moscow State University, 119991 Moscow, Russian Federation,

b) Lebedev Physical Institute of RAS, Leninskiy Prospekt, 53, 119991 Moscow, Russia

[*] *e-mail: melik.nubarov@belozersky.msu.ru*

Table of Contents

S1. Formal kinetics of POCL reaction in the presence of water

Model of POCL reaction in excess of hydrogen peroxide.

The kinetic model in a homogeneous system comprises the following sequence of reactions. At the first stage, a nucleophilic attack of hydrogen peroxide or water on oxalate

ether (I) occurs, which is accompanied by the formation of peroxyoxalate (II) or half-ester of oxalic acid (IV). At the second step, peroxyoxalate intramolecular transformation into 1,2-dioxetedione occurs, which is accompanied by various side processes which do not result in compounds capable of light emission. They include monomolecular or hydrolytic decomposition of peroxyoxalate, or, in excess of H_2O_2, the formation of oxalyl diperoxide (V) also unable to react with the light-emitting activator. Finally, at the third stage, 1,2-dioxetanedione can either reversibly oxidize the activator with subsequent light emission or undergo a decomposition into 2 molecules of carbon dioxide without light emission.

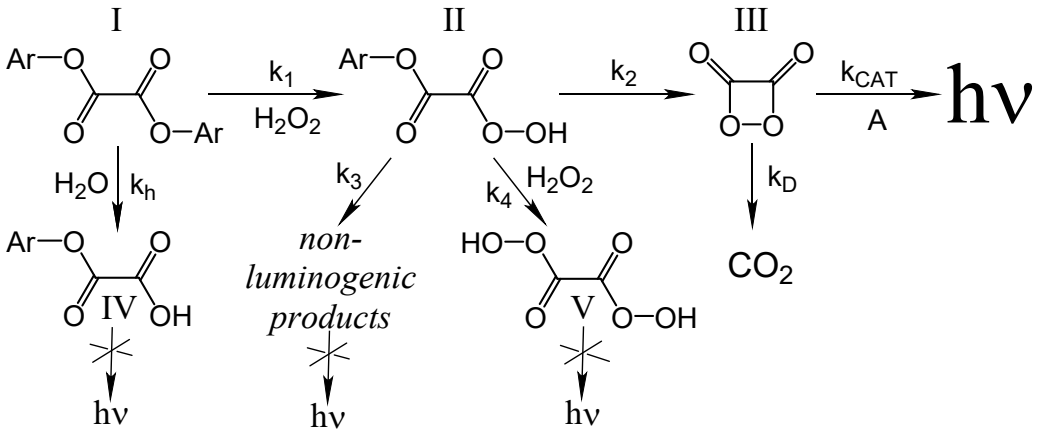

Scheme S1. Scheme of Peroxyoxalate Chemiluminescent Reaction.

We can write the following system of differential equations, where [L] – is the concentration of emitted photons, and concentrations of oxalate, peroxyoxalate, 1,2-dioxetanedione, and hydrogen peroxide are denoted as [Ox], [Perox], [D], and $[H_2O_2]$.

$$\frac{dL}{dt} = \Phi k_{CAT}[D][A]_0 \tag{S1}$$

$$\frac{d[Ox]}{dt} = -k_1[H_2O_2][Ox] - k_h[Ox] \tag{S2}$$

$$\frac{d[Perox]}{dt} = k_1[H_2O_2][Ox] - (k_2 + k_3 + k_4[H_2O_2])[Perox] \tag{S3}$$

$$\frac{d[D]}{dt} = k_2[Perox] - k_{CAT}[A][D] - k_D[D] \tag{S4}$$

Taking into account that the fraction of oxalate entering the reaction with H_2O_2 decreases linearly with decreasing H_2O_2 concentration, only marginal fraction of hydrogen peroxide is consumed in POCL reaction. So, we can accept that $[H_2O_2]$ remains nearly constant throughout the experiment. If so, we can solve eq. (S2) as

$$[Ox] = [Ox]_0 e^{-(k_1[H_2O_2]_0 + k_h)\cdot t} \tag{S5}$$

Then substituting this equation into (S3), we obtain

$$\frac{d[Perox]}{dt} = k_1[H_2O_2]_0[Ox]_0 e^{-(k_1[H_2O_2]_0+k_h)t} - (k_2 + k_3 + k_4[H_2O_2]_0)[Perox] \quad \text{(S6)}$$

To find a partial solution of this equation the time-dependent term should be set to zero and the obtained differential equation is integrated to give:

$$\frac{d[Perox]}{dt} = -(k_2 + k_3 + k_4[H_2O_2]_0)[Perox] \quad \text{(S7)}$$

This equation has the series of solutions in the following form:

$$Ln[Perox] = -(k_2 + k_3 + k_4[H_2O_2]_0)t + LnC_1(t)$$

And potentiating, we obtain $[Perox] = C_1(t)e^{-(k_2+k_3+k_4[H_2O_2]_0)t}$ (S8)

Then,

$$\frac{dC_1(t)}{dt} e^{-(k_2+k_3+k_4[H_2O_2]_0)t} - C_1(t)(k_2 + k_3 + k_4[H_2O_2]_0)e^{-(k_2+k_3+k_4[H_2O_2]_0)t} =$$
$$= k_1[H_2O_2]_0[Ox]_0 e^{-(k_1[H_2O_2]_0+k_3+k_h[H_2O_2]_0)t} - (k_2 + k_3 + k_4[H_2O_2]_0)C_1(t)e^{-(k_2+k_3+k_4[H_2O_2]_0)t}$$

And simplifying, obtain:

$$\frac{dC_1(t)}{dt} = k_1[H_2O_2]_0[Ox]_0 e^{-(k_1[H_2O_2]_0+k_h-k_2-k_3-k_4[H_2O_2]_0)t} \quad \text{(S9)}$$

Then, integrating we obtain the expression for $C_1(t)$

$$C_1(t) = -\frac{k_1[H_2O_2]_0[Ox]_0}{k_1[H_2O_2]_0 + k_h - k_2 - k_3 - k_4[H_2O_2]_0} e^{-(k_1[H_2O_2]_0+k_h-k_2-k_3-k_4[H_2O_2]_0)t} + C_2 \quad \text{(S10)}$$

Which should be applied to (S8):

$$[Perox] = -\frac{k_1[H_2O_2]_0[Ox]_0}{k_1[H_2O_2]_0 + k_h - k_2 - k_3 - k_4[H_2O_2]_0} e^{-(k_1[H_2O_2]_0+k_h)t} + C_2 e^{-(k_2+k_3+k_4[H_2O_2]_0)t}.$$

C_2 can be found assuming that peroxyoxalate is absent at the beginning of the reaction, i.e. *[Perox]=0* at *t=0*:

$$0 = -\frac{k_1[H_2O_2]_0[Ox]_0}{k_1[H_2O_2]_0 + k_h - k_2 - k_3 - k_4[H_2O_2]_0} + C_2, \text{ so}$$

$$C_2 = \frac{k_1[H_2O_2]_0[Ox]_0}{k_1[H_2O_2]_0 + k_h - k_2 - k_3 - k_4[H_2O_2]_0} \quad \text{(S11)}$$

and $$[Perox] = \frac{k_1[H_2O_2]_0[Ox]_0}{k_2 + k_3 + k_4[H_2O_2]_0 - k_1[H_2O_2]_0 - k_h} \left(e^{-(k_1[H_2O_2]_0+k_h)t} - e^{-(k_2+k_3+k_4[H_2O_2]_0)t}\right) \quad \text{(S12)}$$

Introducing three composite constants to simplify the notation:

$$k_2 + k_3 + k_4[H_2O_2] = a$$
$$k_{CAT}[A]_0 + k_D = b$$
$$k_1[H_2O_2]_0 + k_h = c$$

we can write $[Perox] = \frac{k_1[H_2O_2]_0[Ox]_0}{a-c}\left(e^{-ct} - e^{-at}\right)$ (S12a)

We then substitute [Perox] from equation (S12a) into equation (S4) to solve it with respect to the concentration of 1,2-dioxethandione:

$$\frac{d[D]}{dt} = \frac{k_1k_2[H_2O_2]_0[Ox]_0}{a-c}\left(e^{-ct} - e^{-at}\right) - b[D] \quad \text{(S13)}$$

At first, finding a partial solution of equation (S13) we solve it under the condition of *t* tending to infinity: $\frac{d[D]}{dt} = -b[D]$ (S14)

Then $Ln[D] = -bt + LnC_3(t)$, or $[D] = C_3(t)e^{-bt}$. This solution is applied to eq. (S13) to find the time-dependent integration constant $C_3(t)$:

$$\frac{dC_3(t)}{dt}e^{-bt} - C_3(t)be^{-bt} = \frac{k_1k_2[H_2O_2]_0[Ox]_0}{a-c}\left(e^{-ct} - e^{-at}\right) - bC_3(t)e^{-bt} \quad \text{(S15)}$$

which after simplification is reduced to the following:

$$\frac{dC_3(t)}{dt} = \frac{k_1k_2[H_2O_2]_0[Ox]_0}{a-c}\left(e^{-ct} - e^{-at}\right)\cdot e^{bt} \quad \text{(S16)}$$

Integrating, we obtain

$$C_3(t) = \frac{k_1k_2[H_2O_2]_0[Ox]_0}{a-c}\left(\frac{e^{-(c-b)t}}{b-c} - \frac{e^{-(a-b)t}}{b-a}\right) + C_4 \quad \text{(S17)}$$

So, $[D] = \left(\frac{k_1k_2[H_2O_2]_0[Ox]_0}{a-c}\left(\frac{e^{-(c-b)t}}{b-c} - \frac{e^{-(a-b)t}}{b-a}\right) + C_4\right)\cdot e^{-bt}$ (S18)

Then, again assuming that at t=0, [D]=0, we obtain:

$[D] = \left(\frac{k_1k_2[H_2O_2]_0[Ox]_0}{a-c}\left(\frac{e^{-ct}}{b-c} - \frac{e^{-at}}{b-a}\right) + C_4e^{-bt}\right)$ and $C_4 = \frac{k_1k_2[H_2O_2]_0[Ox]_0}{(b-c)(b-a)}$, so

$$[D] = k_1k_2[H_2O_2]_0[Ox]_0\left(\frac{e^{-ct}}{(a-c)(b-c)} - \frac{e^{-at}}{(a-c)(b-a)} + \frac{e^{-bt}}{(b-c)(b-a)}\right) \quad \text{(S20)}$$

$$\boxed{I(t) = \frac{\Phi k_1k_2k_{CAT}[H_2O_2]_0[Ox]_0[A]_0}{(a-c)(b-c)(b-a)}\left((b-a)\cdot e^{-ct} - (b-c)\cdot e^{-at} + (a-c)\cdot e^{-bt}\right)} \quad \text{(S21)}$$

The curve plotted by equation (S21) almost matched the experimental kinetics of the reaction of 0.11 mM 2-PCPO with 4.8 mM H_2O_2 at 0.1 mM perylene as activator in THF/water mixture 8:2

at 6 mM $NaHCO_3$, pH 7.5 (Fig. S1a). This demonstrated that the model satisfactorily describes the kinetics of POCL reaction under conditions of hydrogen peroxide excess.

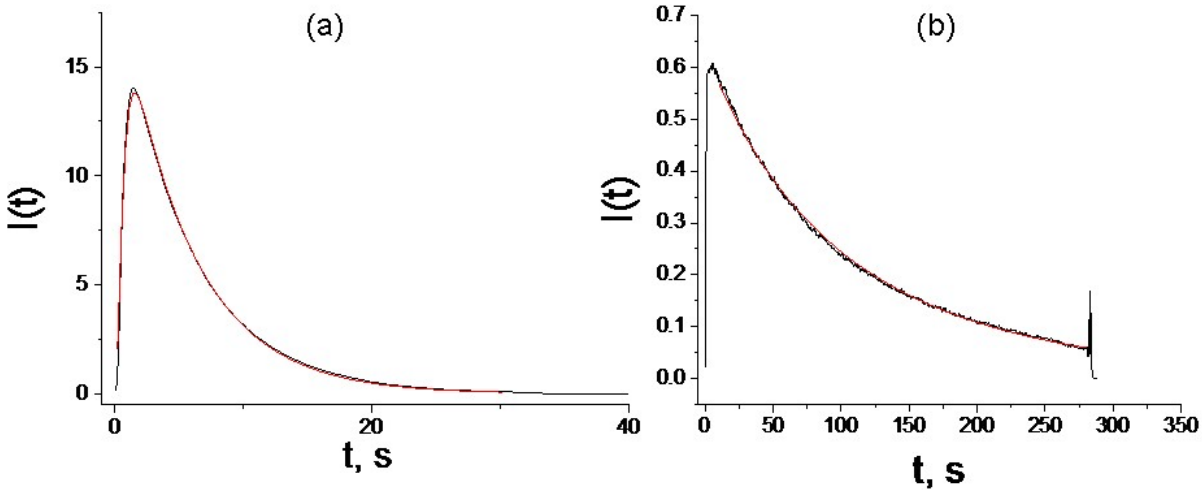

Fig. S1. Testing of kinetic models of POCL reaction under the conditions of an excess ($[H_2O_2]_0$ = 4.8 mM) (a) and a deficiency ($[H_2O_2]_0$ = 0.012 mM) (b) at $[Ox]_0$ = 0.12 mM, and $[A]_0$ = 0.1 mM. Curves 1 (black) - experimental data, and curves 2 (red) – those calculated from eq. S21 (a) and eq. S34 (b).

For the interpretation of the data on the dependence of the integral light intensity on the concentration of hydrogen peroxide, we reintegrated this expression in the interval from 0 to infinity:

$$Q = \frac{\Phi k_1 k_2 k_{CAT} [H_2O_2]_0 [Ox]_0 [A]_0}{abc} \qquad \text{(S22)}$$

or, revealing constants a, b and c

$$\boxed{Q = \frac{\Phi k_1 k_2 k_{CAT} [H_2O_2]_0 [Ox]_0 [A]_0}{(k_2 + k_3 + k_4 [H_2O_2]_0)(k_{CAT} [A]_0 + k_D)(k_1 [H_2O_2]_0 + k_h)}} \qquad \text{(S23)}$$

This equation shows that at low concentrations of H_2O_2 ($k_2 + k_3$? $k_4 [H_2O_2]_0$ and $k_1 [H_2O_2]_0$ = k_h), the integral intensity of chemiluminescence Q should be determined by the ratios $\frac{k_1}{k_h}$ and $\frac{k_D}{k_{CAT}}$.

Model of POCL reaction in the deficiency of hydrogen peroxide

The latter simplification made in the previous section interferes with the constraint $[H_2O_2]_0 \gg [Ox]_0$ made at the very beginning of this modelling. So, in the present section, we considered the case of hydrogen peroxide deficiency in regard to oxalate, so that oxalate is mainly consumed by hydrolysis rather than by POCL reaction.

The system of differential equations that we had to solve in this case was identical to the S1-S4 system discussed above, with the two exceptions, one of which concerns equation S2, which describes oxalate consumption. To describe POCL reaction at low peroxide concentration, the term corresponding to oxalate consumption in POCL reaction was omitted from this equation:

$$\frac{d[Ox]}{dt} = -k_h[Ox] \tag{S24}$$

Another addition to the S1-S4 system was an equation to account for the consumption of hydrogen peroxide due to the peroxyoxalate reaction. We neglected the reaction of H_2O_2 with peroxyoxalate to form oxalyl diperoxide because we considered the region of conditions in which the concentration of peroxide is significantly less than that of oxalate:

$$\frac{d[H_2O_2]}{dt} = -k_1[H_2O_2][Ox] \tag{S25}$$

Thus, the problem was to solve a system involving the equations S1, S24, S3, S4, and S25.

The solution of eq. 24 is

$$[Ox] = [Ox]_0 e^{-k_h \cdot t} \tag{S26}$$

Then substituting this equation into (S25), we obtain

$$\frac{d[H_2O_2]}{dt} = -k_1[H_2O_2][Ox]_0 e^{-k_h \cdot t} \tag{S27}$$

$$Ln\frac{[H_2O_2]}{[H_2O_2]_0} = \frac{k_1[Ox]_0}{k_h}\left(e^{-k_h \cdot t} - 1\right)$$

$$[H_2O_2] = [H_2O_2]_0 e^{-\frac{k_1[Ox]_0}{k_h}\left(1-e^{-k_h \cdot t}\right)} \tag{S28}$$

Since equations S3 and S4 are not homogeneous, an exact analytical integration of such a system is not possible. However, taking into account the literature data [1], it can be assumed that the concentrations of the two intermediates - peroxyloxylate [Perox] and dioxetanedione [D] - become stationary rather quickly during the reaction. Then:

$$\frac{d[Perox]}{dt} = 0 \tag{S29}$$

$$\frac{d[D]}{dt} = 0 \tag{S30}$$

Then substituting the conditions S29 and S30 into equations S3 and S4, correspondingly, we obtain

$$[Perox] = \frac{k_1[H_2O_2]_0[Ox]_0}{k_2 + k_3 + k_4[H_2O_2]_0} e^{-\frac{k_1[Ox]_0}{k_h}\left(1-e^{-k_h t}\right)-k_h t} \quad \text{(S31)}$$

$$k_2[Perox] = k_{CAT}[A]_0[D] + k_D[D] \quad \text{(S32)}$$

$$[D] = \frac{k_1 k_2[H_2O_2]_0[Ox]_0 e^{-\left(\frac{k_1[Ox]_0}{k_h}\left(1-e^{-k_h \cdot t}\right)+k_h \cdot t\right)}}{\left(k_{CAT}[A]_0 + k_D\right)(k_2 + k_3 + k_4[H_2O_2]_0)} \quad \text{(S33)}$$

$$\boxed{I(t) = \frac{\Phi k_1 k_2 k_{CAT}[H_2O_2]_0[Ox]_0[A]_0 e^{-\left(\frac{k_1[Ox]_0}{k_h}\left(1-e^{-k_h t}\right)+k_h \cdot t\right)}}{\left(k_{CAT}[A]_0 + k_D\right)\left(k_2 + k_3 + k_4[H_2O_2]_0\right)}} \quad \text{(S34)}$$

To elucidate the expression for integral chemiluminescence intensity, we integrated this equation by time from zero point to infinity:

$$Q = \frac{\Phi k_2 k_{CAT}[H_2O_2]_0[A]_0\left(1 - e^{-\frac{k_1[Ox]_0}{k_h}}\right)}{\left(k_{CAT}[A]_0 + k_D\right)\left(k_2 + k_3 + k_4[H_2O_2]_0\right)}. \quad \text{(S35)}$$

Denoting the term corresponding to the efficiency of peroxyoxalate transformation into 1,2-dioxetanedione $\frac{k_2}{k_2 + k_3 + k_4[H_2O_2]_0}$ as χ, we obtain

$$Q = \frac{\Phi \chi k_{CAT}[H_2O_2]_0[A]_0\left(1 - e^{-\frac{k_1[Ox]_0}{k_h}}\right)}{\left(k_{CAT}[A]_0 + k_D\right)}$$

At low concentrations of hydrogen peroxide, k_2 ? $k_4[H_2O_2]$. Thus, under conditions of chemiexcited PDT,

$$Q = \frac{\Phi \chi k_{CAT}[A]_0[H_2O_2]_0\left(1 - e^{-\frac{k_1[Ox]_0}{k_h}}\right)}{\left(k_{CAT}[A]_0 + k_D\right)} \quad \text{(S36)}$$

So, when oxalate hydrolysis occurs more rapidly than peroxyoxalate reaction, $\frac{k_1[Ox]_0}{k_h}$ = 1, and the approximation $1 - e^{-\frac{k_1[Ox]_0}{k_h}} \sim \frac{k_1[Ox]_0}{k_h}$ is fulfilled,

$$\boxed{Q \approx \Phi \cdot \chi \cdot \frac{k_1}{k_h} \cdot \frac{k_{CAT}[A]_0}{(k_{CAT}[A]_0 + k_D)} \cdot [H_2O_2]_0[Ox]_0}. \quad \text{(S37)}$$

Thus, at low hydrogen peroxide concentrations, the integral intensity of oxalate chemiluminescence is determined by the ratio of the rate constants of its reactions with hydrogen peroxide and water. The curve plotted by equation (S34) almost matched the experimental kinetics of the reaction of 0.11 mM 2-PCPO with 10 μM H_2O_2 at 0.1 mM perylene as activator in THF/water mixture 8:2 at 6 mM $NaHCO_3$, pH 7.5 (Fig. S1b). This demonstrated that the model satisfactorily describes the kinetics of POCL reaction under conditions of hydrogen peroxide deficiency.

S2 Synthesis of 2-pentyl-oxycarbonyl phenol and 4-pentyl-oxycarbonyl phenol and the corresponding oxalates.

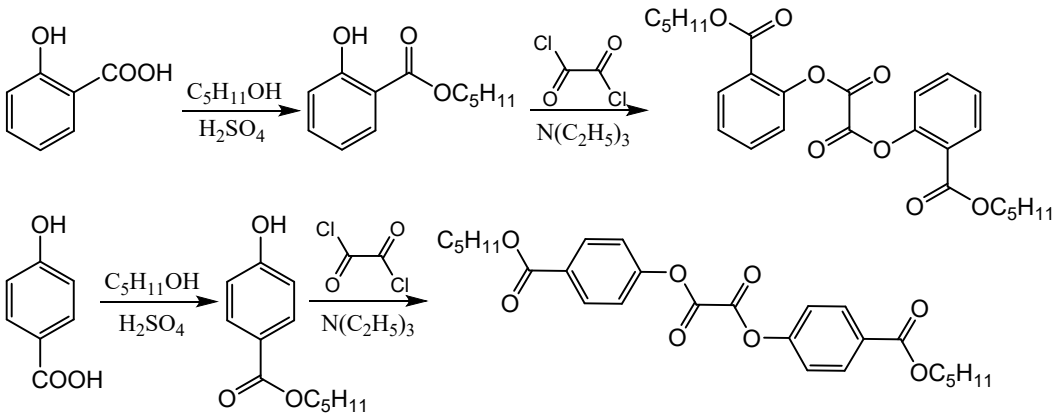

Fig. S2. Scheme of synthesis of pentyl esters of salicylic and 4-hydroxybenzoic acids and the corresponding oxalates.

Synthesis of pentyl esters of salicylic and 4-hydroxybenzoic acids[2]

A 250 mL round-bottom reaction vessel was charged with 30 g (0.217 mol) of salicylic or 4-hydroxybenzoic acid (Sigma, USA), 120 mL (1.1 mol) of the freshly distilled n-pentanol (b.p. 138.5 °C at atmospheric pressure, Komponent-Reaktiv, Russia) and 1.2 mL of sulfuric acid as a catalyst. The mixture was heated in an oil bath with Dean-Stark trap under reflux for about 5 h at 150 °C and then n-pentanol excess was removed by distillation in vacuum of water-jet pump. The residue was washed twice with equal volume of 10% K_2CO_3, diluted with 50 mL of ether and dried over anhydrous sodium sulfate overnight. Then ether was removed on a rotary evaporator (Heidolph, Germany) under reduced pressure and the pentyl esters of salicylic and 4-hydroxybenzoic acids were distilled at about 1-2 Torr on oil bath at 125 ° and 200 °C, respectively. Yields were 85% and 25% for 2- and 4-pentyl-oxycarbonylphenols, respectively. ^{1}H NMR spectra are presented at Fig. S3 and S4. All NMR spectra were recorded using Bruker DRX500

spectrometer with proton precessional frequency 600.13 MHz. Chemical shifts were calibrated using signals of residual protons of the solvent.

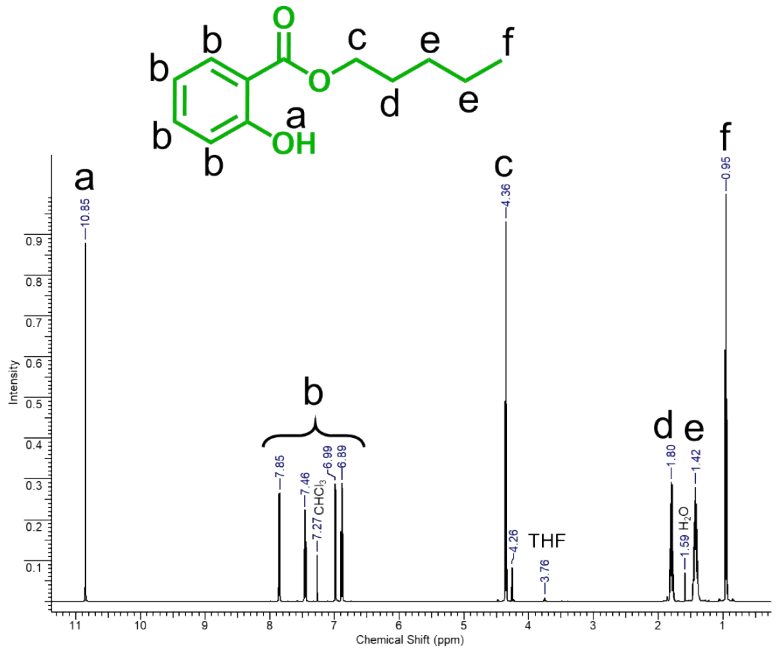

Fig. S3 ^{1}H NMR spectrum (600 MHz) of 2-pentyl-oxycarbonylphenol in $CDCl_3$.

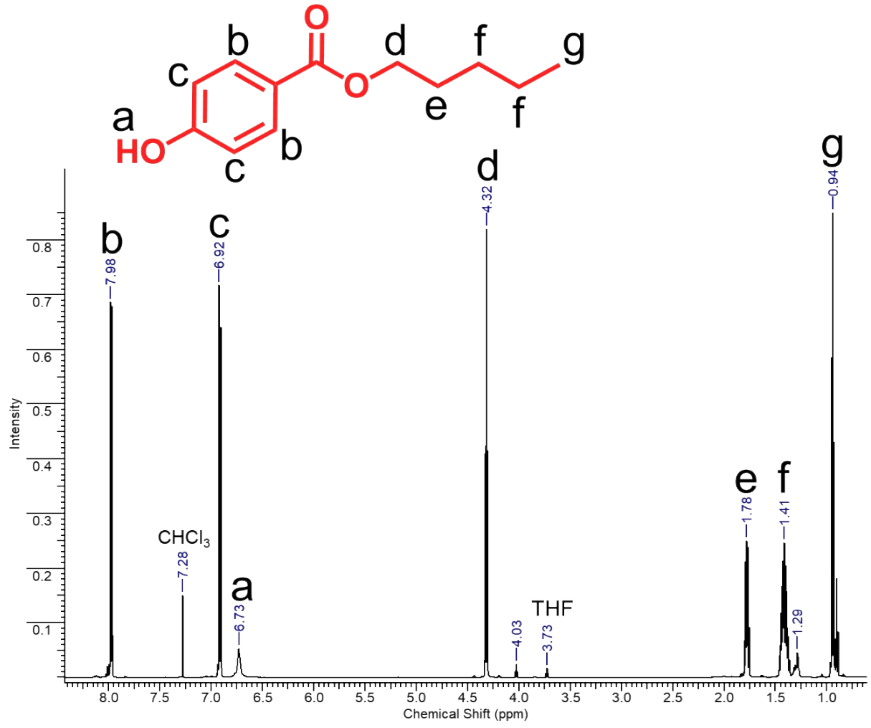

Fig. S4 ^{1}H NMR spectrum (600 MHz) of 4-pentyl-oxycarbonylphenol in $CDCl_3$.

Synthesis of oxalates 2-PCPO and 4-PCPO and their characterization

A 100 mL round-bottom bulb was charged with 1.5 g (7 mmol) of 2- or 4-pentyl-oxycarbonylphenol and 1 mL (7 mmol) of the freshly distilled over CaH_2 triethylamine (Sigma, USA) dissolved in 40 mL of the freshly distilled over sodium metal benzene. The bulb was placed

in water bath at 20 °C and 0.3 mL oxalyl chloride (3.5 mmol) in 40 mL of benzene were added dropwise during about 80 min. After adding the entire amount of oxalyl chloride, the reaction mixture was stirred for 1 h, after which the benzene was evaporated at the rotary evaporator and dissolved in 50 mL chloroform. The raster was washed first with an equal volume of water, then with an equal volume of 1 M hydrochloric acid, and then again three times with an equal volume of water. It was left to dry overnight over sodium sulfate. The chloroform was then evaporated and dissolved in a minimum volume of benzene under heating. Crude oxalate was precipitated with a 4-fold excess of hexane at 10 °C. The precipitate was washed with hexane twice to give white crystals. The residual hexane was removed in a vacuum desiccator overnight. ^{1}H NMR spectra of 2- and 4-PCPO, as well as BPO synthesized as described elsewhere [3] are presented in Figures S5-S7.

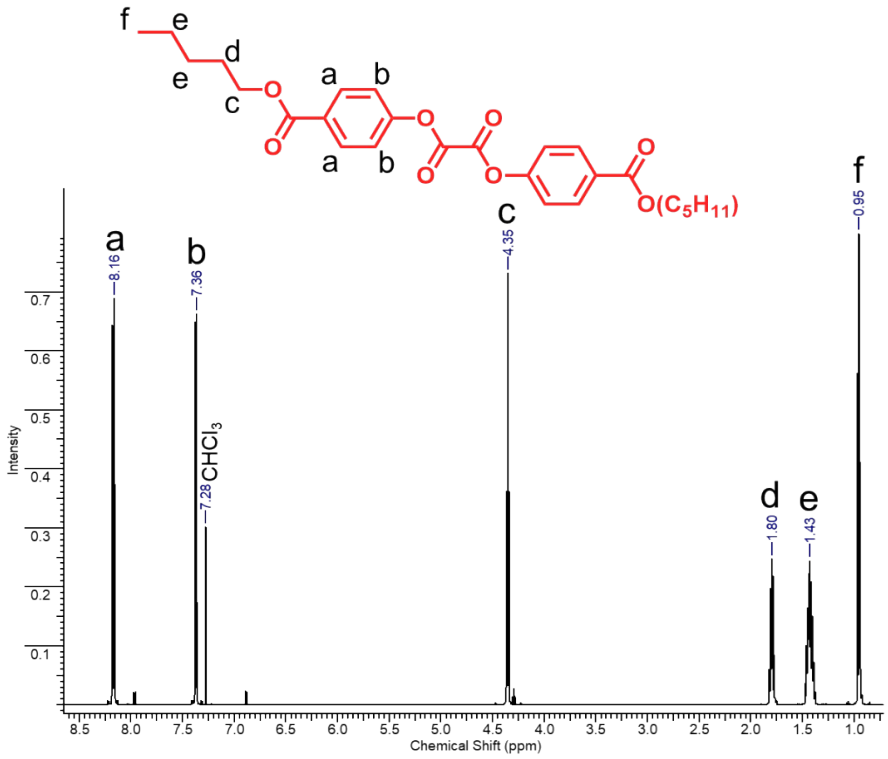

Fig. S5 ^{1}H NMR spectrum of 4-PCPO in $CDCl_3$.

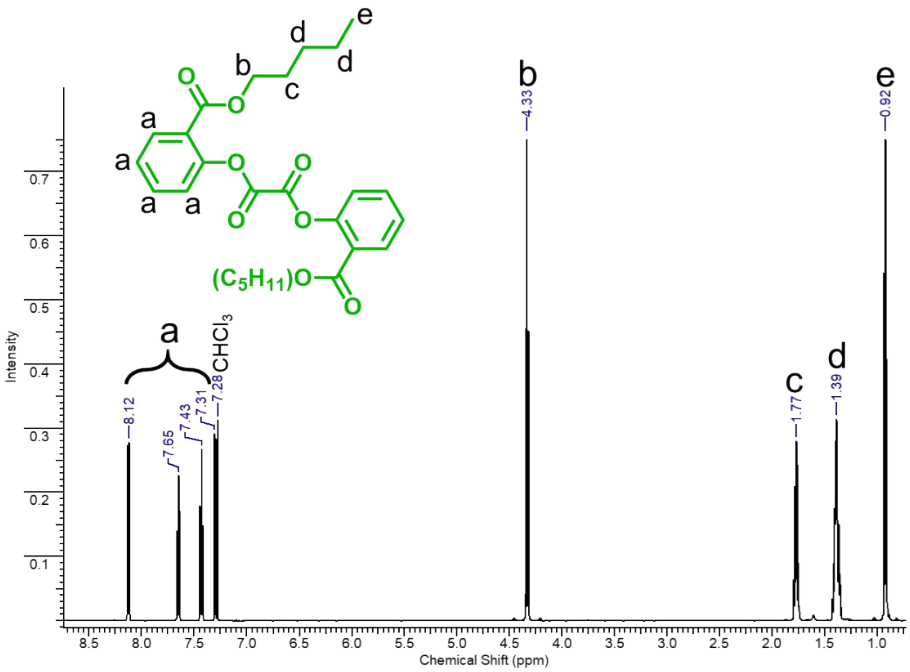

Fig. S6 ^{1}H NMR spectrum of 2-PCPO in $CDCl_3$.

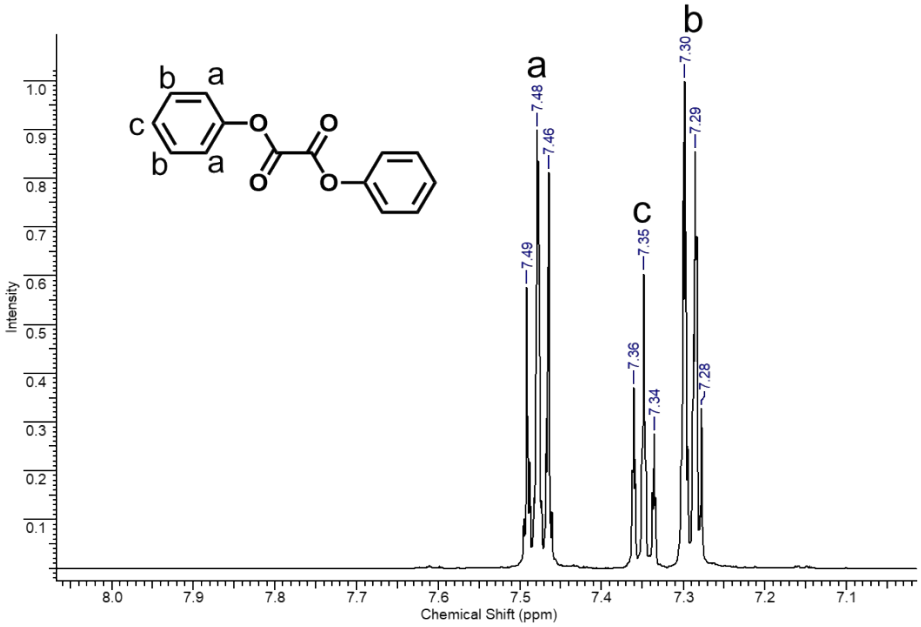

Fig. S7 ^{1}H NMR spectrum of bis(phenyloxalate) in $CDCl_3$.

S3 Spectrophotometric titration

10-25 mM solutions of oxalate or the corresponding phenol in THF were diluted 100-fold in 15 mM NaOH to ensure complete dissolution of the sample. The solution was additionally diluted 2-5-fold with distilled water until a solution with absorbance falling within the range of the highest accuracy of spectrophotometric measurements (0.5-1.1 absorbance units) was obtained. The final phenol concentration in the samples varied between 0.05 and 0.125 mM. The solutions were titrated with 0.1 M HCl and pH and UV-spectra were recorded using Akvilon pH-420 pH-meter

with microelectrode and Ultrospec 1100 Pro spectrophotometer (Amersham, Great Britain) (Fig. S8).

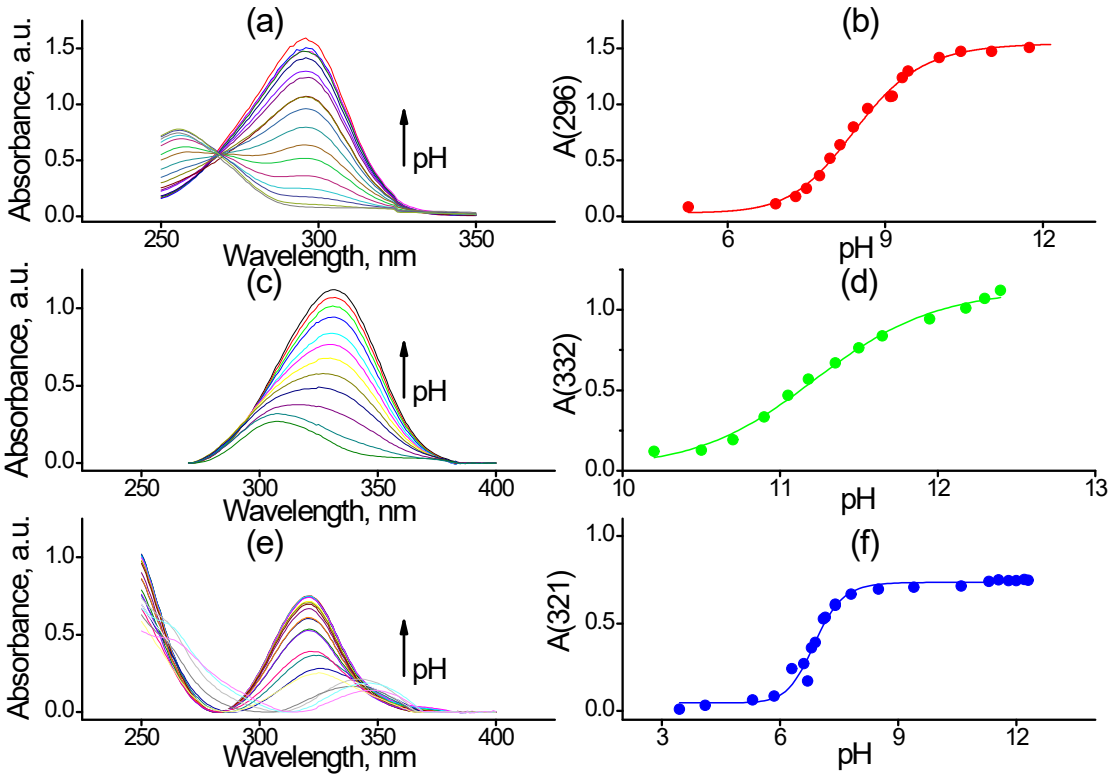

Fig. S8 (a) UV spectra of 0.05 M 4-pentyl-oxycarbonylphenol (4-PCP) in water upon pH change from 12 to 3.5. (b) pH dependence of 4-PCP absorbance at wavelength 296 nm, corresponding to the deprotonated form of phenol; (c) UV spectra of 0.1 M 2-pentyl-oxycarbonylphenol (4-PCP) in water as pH decreases; (d) pH dependence of 2-PCP absorbance at wavelength 332 nm responding to the deprotonated form of phenol; (e) UV-vis spectra change of 0.05 M 3,4,6-trichloro-2-pentyl-oxycarbonylphenol (CPP) in water upon pH change from 12 to 3.5. (f) pH dependence of 4-PCP absorbance at wavelength 321 nm responding to the deprotonated form of phenol.

S4. ^{13}C NMR spectra of the oxalates

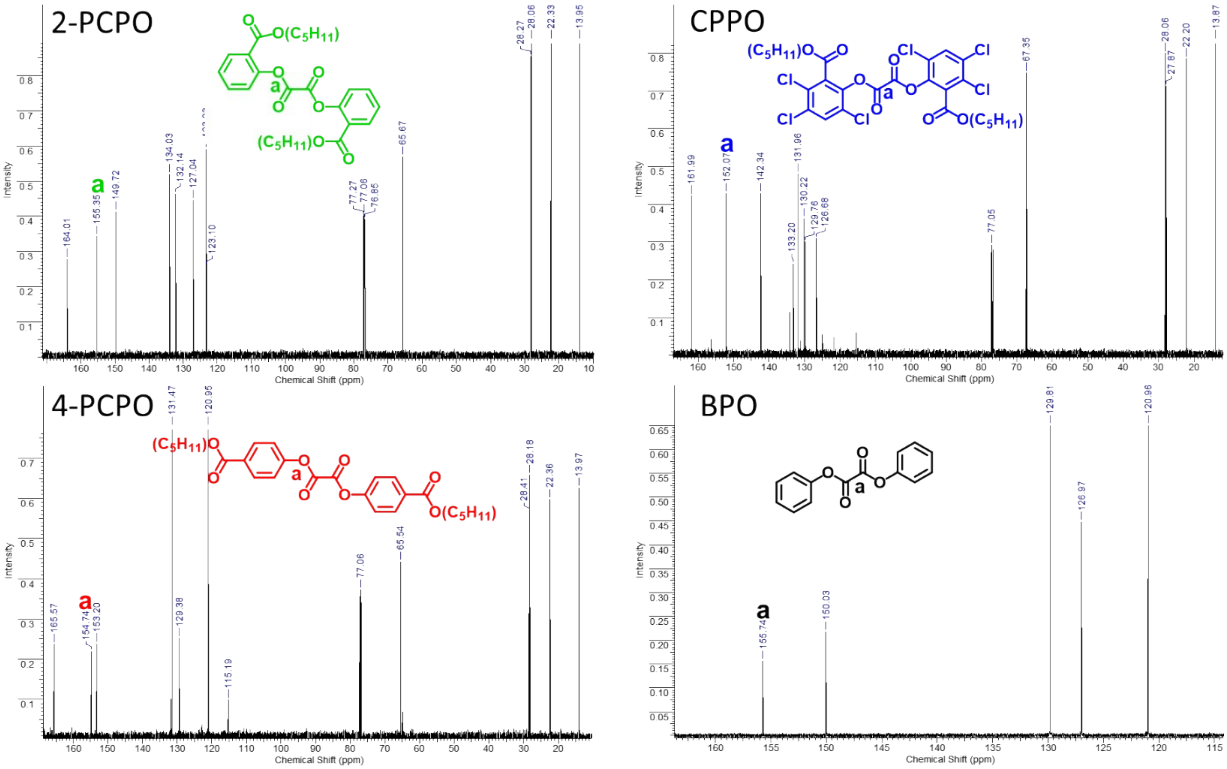

Fig. S9. ^{13}C NMR spectra of the studied oxalates in $CDCl_3$.

S5. Neuvonen and Neuvonen scale of electron deficiency in esters

Following H. Neuvonen and K. Neuvonen, we used the chemical shift values of carbonyl carbons in ^{13}C NMR as independent experimental data on partial charges on carbonyls of oxalate group. Indeed, since the screening constant of each atom depends directly on the partial charge on this atom, the chemical shift can be considered as information about the partial charge on this atom. H. Neuvonen and K. Neuvonen has previously shown that the hydrolysis rate constants of substituted aryl dichloroacetates correlate well with the chemical shifts of carbonyl carbons, with the partial charge on the carbon atom increasing as the chemical shift decreases [4]. (Fig. S10a) Using previously reported data on ^{13}C NMR of some oxalates, we have constructed a similar correlation between the chemistry shift of the C=O groups of oxalates and the pKa of the leaving group. As in the case of dichloroacetates, chemical shifts of C=O carbons of oxalates also decreased when electronegativity of phenyl substituents grew up. (Table S1 and Fig. S10b)

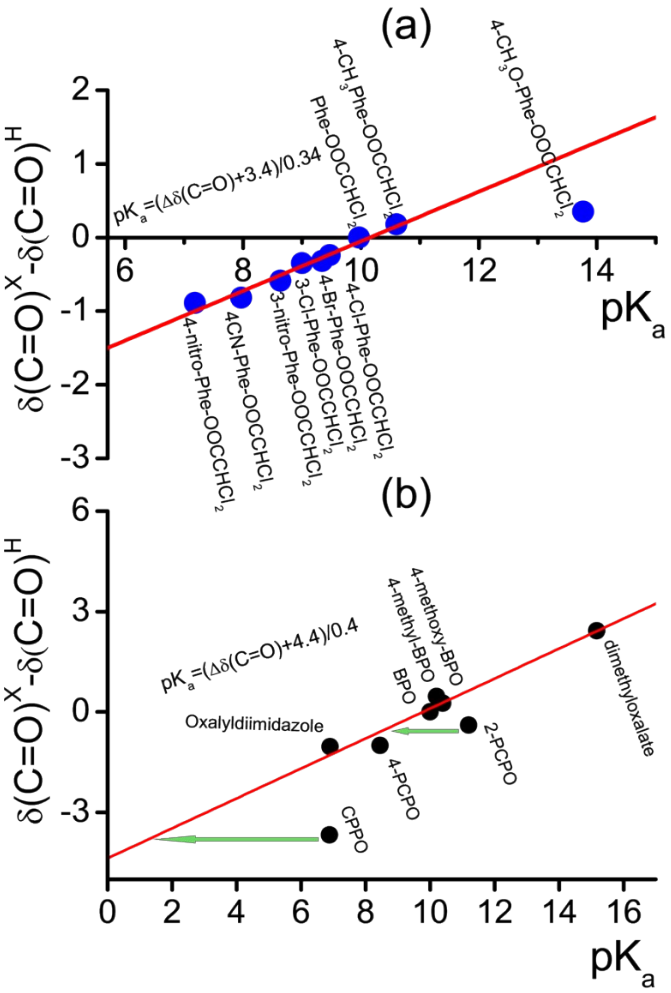

Fig. S10. Relationship between ^{13}C NMR chemical shifts of carbonyl carbons and leaving group pK_a in substituted phenyl dichloroacetates (a) and oxalic acid derivatives (b).

At the same time, the chemical shifts of carbonyl carbons in CPPO and 4-PCPO were noticeably smaller than the chemical shift of C=O groups in BPO. The chemical shift of the carbonyl group of 2-PCPO turned out to be very close to that of 4-PCPO. The oxalates 2-PCPO and CPPO with carbonyl groups at o-position deviate to the right from this correlation that is ascribed to the strong overestimation of pK_a of salicylate phenolic hydroxyls. Interestingly, the data on the chemical shifts of oxalate (this work) and dichloroacetate esters are described by similar empirical equations (see in the graph) indicating that common structural causes underlie these relationships.

Table S1. Relationship between ^{13}C NMR chemical shifts of carbonyl carbons and leaving group pKa in oxalic acid derivatives

Compound	Δδ(C=O), ppm	pK_a	ref.
BPO	0	10	This work
2-PCPO	-0.39	11.2	This work
4-PCPO	-1	8.45	This work
CPPO	-3.67	6.88	This work
methoxy-phenyloxalate	0.26	10.4	[5]
methyl-phenyloxalate	0.46	10.2	[2]
Dimethyloxalate	2.43	15.17	[6]
Oxalic acid	6.56	14	[7]
Oxalyldiimidazole	-1.04	6.9	[8]

S6. Measurement of POCL reaction kinetics in homogenous THF/water buffer

Kinetics of POCL reaction and integral chemiluminescence intensity in THF/water system were analysed as follows. Oxalate and perylene solutions in 1.6 mL of THF were placed in the cuvette and equilibrated at 37 ^oC for about 3-5 min. The reaction was initiated by injection of 0.4 mL of 20 mM H_2O_2 in 30 mM $NaHCO_3$, pH 7.5 equilibrated at 37 ^oC. If not otherwise stated, the initial perylene, oxalate, and H_2O_2 concentration were 0.1 mM, 0.11 mM, and 4.8 mM, respectively. Typical reaction kinetics is shown in Fig S1. Chemiluminescence was recorded using a Hitachi 650-10S fluorimeter at a wavelength of 440 nm and emission slit of 20 nm with the light source turned off.

Kinetics of hydrolysis (a) and the reaction with 4.8 mM hydrogen peroxide (b) of BPO (1), 2-PCPO (2), 4-PCPO (3), and CPPO (4) are shown in Fig. S11a. By the rate constants of hydrolysis, the investigated oxalates were arranged in a completely different order than by sensitivity to hydrogen peroxide, although similar mechanisms underlie their reactions with hydrogen peroxide and water. 4-PCPO exhibited the highest hydrolysis rate and its ortho-isomer, 2 -PCPO, exhibited the highest stability. At the same time, oxalates containing the most and least electron deficient phenols - CPPO and BPO - showed close to each other and intermediate in absolute value hydrolysis rates in aqueous-organic medium THF/water 8:2.

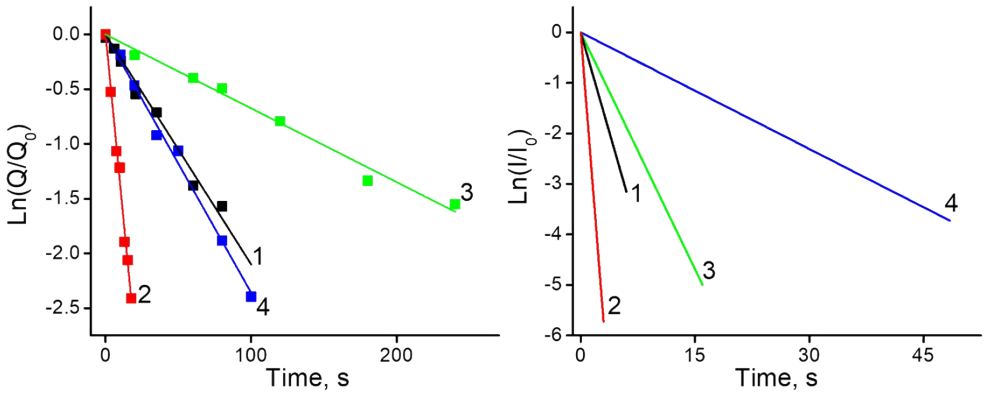

Fig. S11. Kinetics of hydrolysis (a) and POCL reaction (b) of BPO (1), 4-PCPO (2), 2-PCPO (3), and CPPO (4) in homogenous THF/water (8:2) solution.

S7. Evaluation of oxalates sensitivity under acidic conditions.

To estimate the sensitivity of POCL reaction under acidic conditions, the experiments described in Section 6 were repeated according to the same protocol, except the carbonate buffer pH 7.5 was replaced for 30 mM $NaOOCCH_3$, pH 5.5. The integral intensities of all oxalates except CPPO measured at pH 5.5 were 30-50% less than those determined at pH 7.5 (Fig. S12a). The drop in sensitivity with decreasing pH in the case of the most electronegative CPPO was even more significant and amounted to about 90%.

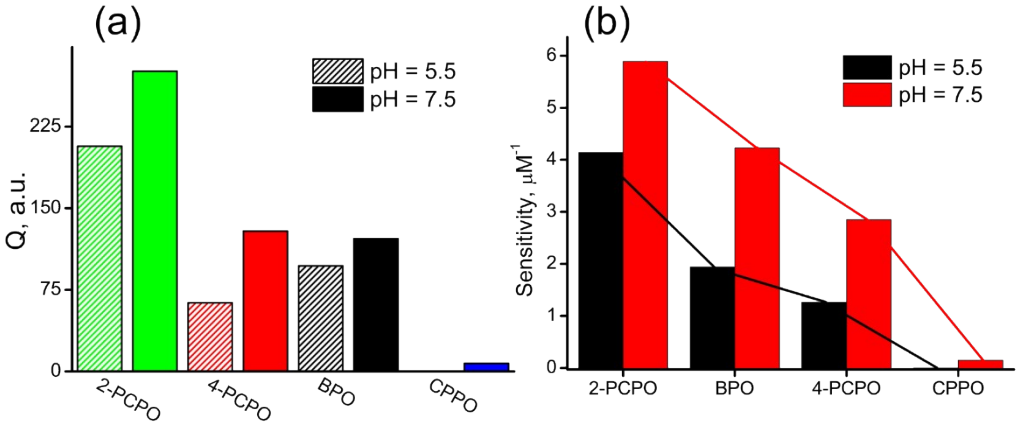

Fig. S12. (a) Integral intensities of POCL reaction under neutral (pH 7.5, filled bars) and slightly acidic (pH 5.5, hatched bars) conditions at concentrations of oxalate 0.11 mM, perylene 1 mM, H_2O_2 4.8 mM in THF/water 8:2 mixture. Buffer concentration in both cases was 30 mM per water part. (b) Sensitivities of POCL reaction with different oxalates at pH 5.5 (red) and 7.5 (black). Lines are drawn as a guide for eyes.

A decrease in pH should slow down the reactions of all the oxalates under study with both hydrogen peroxide and water, as well as the cyclisation (k_2) and decomposition (k_3 and k_4) of peroxyoxalate. Therefore, we cannot say whether the decrease in oxalate activity with a decrease in pH is a consequence of a more significant slowdown in the reaction of oxalates with hydrogen peroxide (k_1), or intramolecular cyclization (k_2) compared to the hydrolysis of the initial oxalate (k^h) or decomposition of peroxyoxalate. At the same time, the ranking of oxalates according to their sensitivity to peroxide remained unchanged when the pH decreased

S8. Direct and extrapolation methods of k_h measurement.

Determination of the hydrolysis constant by extrapolation of the observed constant of chemiluminescence decay to zero H_2O_2 concentration according to the protocol used in [9] gave results similar to those obtained by direct measurements of the rate of oxalate hydrolytic decomposition during its incubation in an aqueous-organic solution. (Fig. S11) At the same time, the need for a long-range extrapolation makes this approach less accurate for k_h estimation. Therefore, routinely, we used the method of direct determination of hydrolysis rate constant as a difference between k_{obs} and k_h. The values of k_1 and k_h determined using regression technique from k_{obs} as a function of H_2O_2 concentration were of $(35 \pm 2)\times10^{-6}$ $M^{-1}\cdot s^{-1}$ and $(5.3 \pm 1.1)\times10^{-3}$ s^{-1}, correspondingly. These values are close to the values presented in Table 1 in the main text.

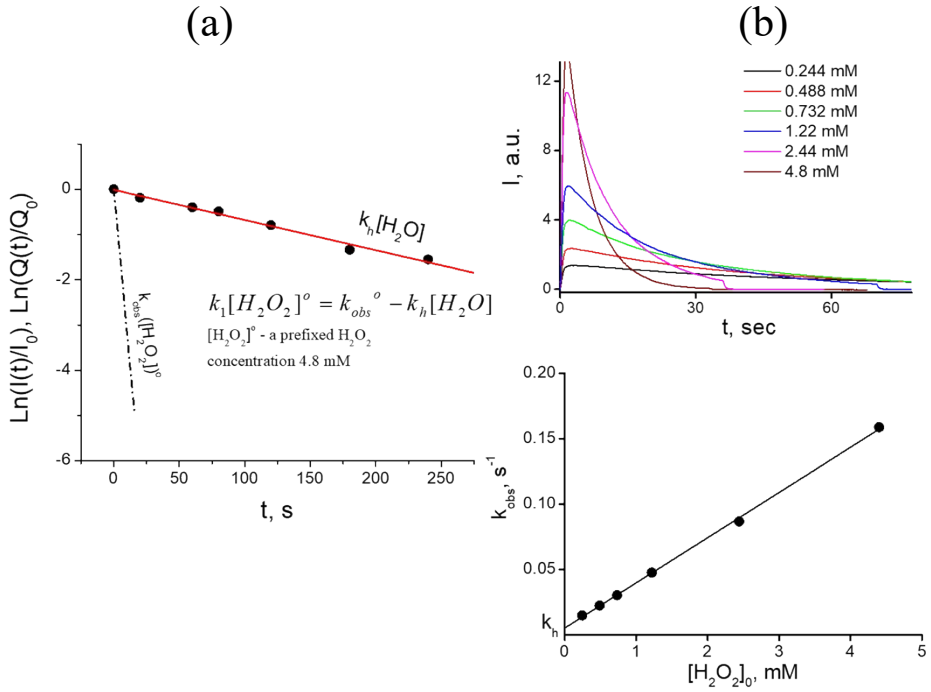

Fig. S13. Comparison of direct and extrapolation methods of k_h determination. (a) Kinetics of 2-PCPO hydrolysis in THF/water (8:2) mixture (red curve) and its reaction with hydrogen peroxide (back curve) under standard conditions at a prefixed concentration of H_2O_2 of 4.8 mM

(Section S7 in ESI). (b) Kinetics of chemiluminescence emission during 2-PCPO reaction with different concentrations of H_2O_2 shown in the plot.

S9. Protocol of synthesis of $mPEG_{90}$-$PLLA_{110}$.

Monomethoxy polyethylene oxide 4000 (TCI, Japan) was dried by azeotropic distillation with anhydrous benzene. L-lactide (Sigma-Aldrich) was recrystallized from anhydrous ethyl acetate.

The required amount of mPEG was added to a 50 mL Schlenk flask and transferred into an oil bath at 100 °C, connected to a vacuum line and vacuumized until the melt stops boiling. Then we fill the flask with argon and introduce the required amount of lactide. The flask is heated to 130 °C and the cycle of pumping-filling with argon is performed three times. After that we introduced tin octanoate catalyst (0.2 equivalent of mPEG). Then the argon pumping-filling procedure was repeated once. The polymerization was carried out for 3 hours. After cooling of the reaction mixture, the solid product was dissolved in a minimum volume of boiling THF. The resulting solution was centrifuged at 2000 rpm for 10 minutes to separate from SnO_2 impurity, separating the precipitate by decanting, and a 10-fold excess of ether was added to the resulting solution. The white precipitate was separated by centrifugation at 2000 rpm for 10 minutes. This procedure was repeated twice. To remove traces of THF, the precipitate was washed with ether, centrifuged and dried in a vacuum desiccator overnight. The obtained polymer was analyzed by ^{1}H NMR and GPC.

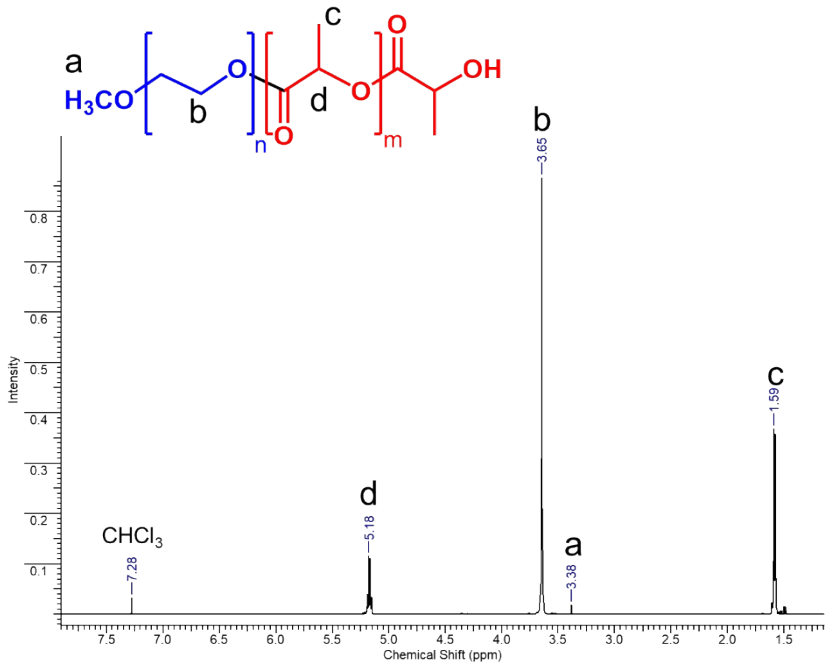

Fig. S14 ^{1}H NMR spectrum (600 MHz) of $mPEG_{90}$-$PLLA_{110}$ block copolymer in $CDCl_3$.

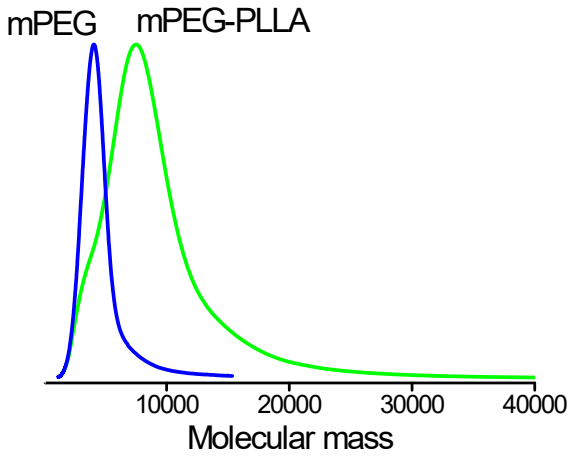

Fig. S15. Analysis of molecular weight distribution of $mPEG_{90}$-$PLLA_{110}$ block copolymer with GPC.

S10. Dynamic Light scattering analysis of $mPEG_{90}$-$PLLA_{110}$ micelles

Mean hydrodynamic radii and size distribution of thus formed micelles was analyzed using the PhotoCor scattered laser light goniometer (PhotoCor Corp., USA) equipped with a He-Ne laser (λ = 633 nm, 15 mW) as a light source. The autocorrelation functions of scattered light intensity fluctuations (ACF) were measured at an angle 90° using a 288-channel PhotoCor-SP correlator with a logarithmic time scale from 2.5×10^{-8} to 6800 s. Data collection for obtaining ACF was carried out for 5-20 minutes depending on the intensity of the scattered light. ACF analysis was performed by the regularization method using the DynaLS software (PhotoCor Corp., USA) to obtain the distributions of diffusion coefficients for scattering particles. The values R_h of the hydrodynamic diameter were calculated using the Stokes equation in the approximation of spherical particles.

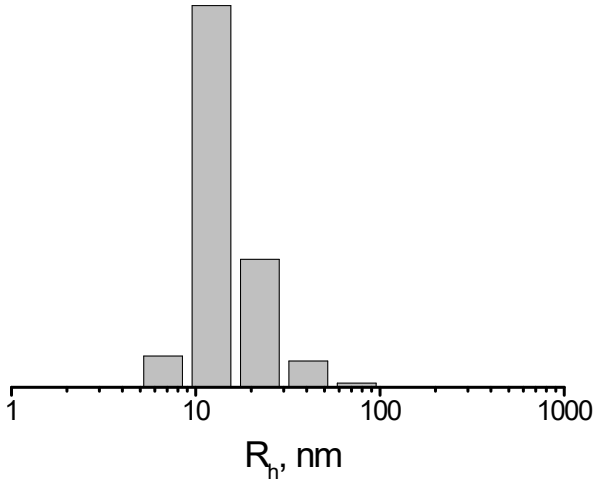

Fig. S16. Mass average distribution of $mPEG_{90}$-PLA_{110} block copolymer micelles by hydrodynamic radii in PBS obtained by Dynamic Light Scattering at 37 °C. Mean average hydrodynamic radius was 22 nm.

S11. Evaluation of the extent of solubilisation of the Solubilized of component reaction in $mPEG_{90}$-$PLLA_{110}$ block copolymer micelles

The extent of solubilization of perylene in block copolymer micelles was evaluated by the changes in its fluorescence upon addition of increasing concentrations of $mPEG_{90}$-$PLLA_{110}$ block copolymer. The concentration of perylene in the final solution was 0.01 mM, and the concentration of polymer was varied from 1.2 mg/mL to 11.8 mg/mL. Fluorescence was recorded using a Hitachi 650-10S fluorimeter within the 430 – 600 nm range of wavelengths and excited at 420 nm. Nearly 80% solubilisation of perylene was achieved at 2.5 mg/mL of the copolymer.

The extent of solubilization of oxalate in the block copolymer micelles was determined by measuring the integral intensity of POCL reaction at different concentration of block copolymer. To this end, we added 50 μL of 5 mM oxalate and 20 μL of 1 mM perylene solutions in THF to the solution of a required amount of $mPEG_{90}$-$PLLA_{110}$ block copolymer in 150 μL THF and thoroughly stirred continuously during 5 min to achieve better reproducibility. The micelles were formed by addition of 0.4 mL of PBS during intensive stirring on Vortex mixer during 10 s, then 0.6 mL of PBS were added during continuous stirring during additional 10 s, and finally 1 mL of PBS was added, mixed thoroughly and transferred to a cuvette. POCL reaction was initiated by injecting the required amount of hydrogen peroxide. Chemiluminescence was recorded using a Hitachi 650-10S fluorimeter at a wavelength of 440 nm and emission slit of 20 nm with the light source turned off.

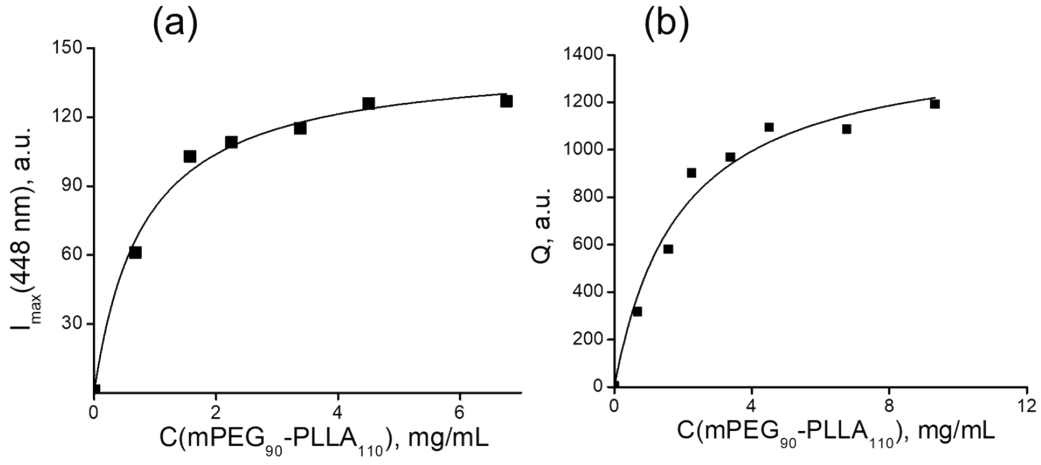

Fig. S17. (a) Change in the maximum fluorescence intensity of perylene at 448 nm at different polymer concentrations and (b) change in the integrated intensity of PO reaction at different polymer concentrations in the presence 0.01 mM perylene and 0,11 mM 4-PCPO.

Figure S17a shows the dependence the fluorescence intensity of perylene on polymer $mPEG_{90}$-$PLLA_{110}$ concentration. Increase in fluorescence intensity was observed with increasing polymer concentration due to enhancement of solubilization degree. The fluorescence intensity

increased at $mPEG_{90}$-$PLLA_{110}$ concentrations up to 1.8-2 mg/mL indicating gradual solubilization of perylene in the core of the polymer micelles. Further increase in polymer concentration does not significantly increase fluorescence intensity. Formally assuming that the plateau on the curve corresponds to complete solubilization, we can say that at a polymer concentration of 2.5 mg/mL, solubilization is about 90%. However, with a significant degree of certainty, we can say that this value is underestimated. The fact is that perylene is almost insoluble in water. Therefore, even at the lowest polymer concentration, it is quantitatively partitioned into micelles, but due to the very high local concentration, its fluorescence is low. As the polymer concentration in the sample increases, the local concentration of perylene decreases and its fluorescence grows up.

A similar pattern is observed for the solubilization of a mixture of 4-PCPO oxalate and perylene (Fig. 17b). Both components are insoluble in water (LogPwater/octanol = 8.2 and 6.4, correspondingly). Therefore, the increase in fluorescence as the polymer concentration increases between 0.1 and 2 mg/mL should most likely be explained by a decrease in the local concentration of the activator and the resulting increase in its fluorescence. Thus, our available data on the solubilization of perylene and the effect of polymer concentration on the integrated chemiluminescence intensity indicate almost quantitative solubilization of oxalates and preylene at a $mPEG_{90}$-$PLLA_{110}$ polymer concentration of 2.5 mg/mL.

S12. Kinetics of POCL reaction and hydrolysis in $mPEG_{90}$-$PLLA_{110}$ block copolymer micelles

The integral intensity of POCL reaction was measured as described in Section 11, using constant block copolymer concentration of 2.5 mg/mL.

To evaluate kinetic constants of micelle-encapsulated oxalate hydrolysis, the micellar nanoreactors were prepared as described above. The reaction mixture was kept in a dry thermostat (37^{o}C) for definite time intervals. Then it was transferred to a cuvette and POCL reaction was initiated by injecting 0.08 mL of 0.1 mol/L of hydrogen peroxide.

Kinetic constants of peroxyoxalate reaction were evaluated at the prefixed concentration of hydrogen peroxide of 4.8 mM for easy comparison of the obtained data with those for the homogeneous THF/water 8:2 solution.

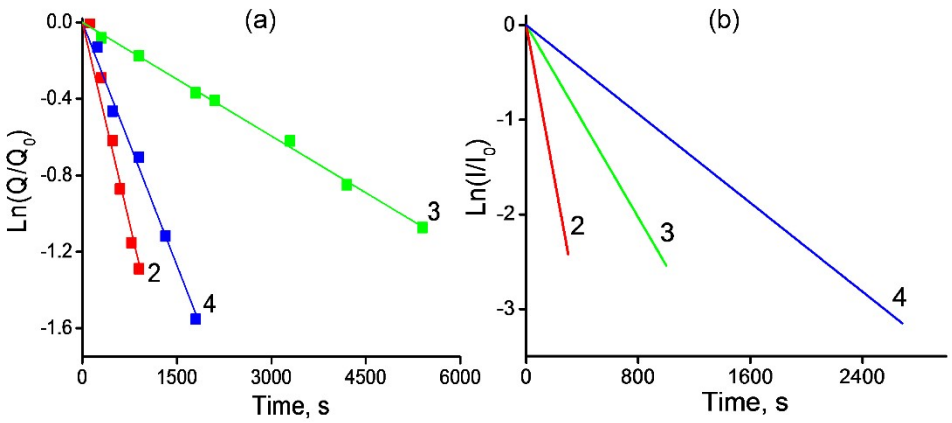

Fig. S18. Kinetics of hydrolysis (a) and POCL reaction (b) of BPO (1), 4-PCPO (2), 2-PCPO (3), and CPPO (4) encapsulated in the 2.5 mg/mL dispersion of $mPEG_{90}$-$PLLA_{110}$ micelles. Concentration of perylene, oxalate and hydrogen peroxide were 0.1 mM, 0.11 mM, and 4.8 mM, correspondingly, PBS, 37 °C.

S 13. Cytotoxicity of the oxalates encapsulated in $mPEG_{90}$-$PLLA_{110}$ micelles

Oxalate toxicity was tested on attached human ovarian adenocarcinoma cells of the multidrug-resistant [10] NCI/ADR-RES (old name MCF-7/ADR[11]) line. Cells were cultured in Nunc plastic vials (Nunclon, Denmark) in DMEM medium containing 4 mM glutamine, 100 μg/mL streptomycin, 100 units/mL penicillin and 10% fetal bovine serum (complete medium) in a CO_2 incubator (NAPCO) at 37ºC in an atmosphere of 5% CO_2 and 95% humidity. On the day before the experiment, cells were seeded in a 96-well plate at 4 thousand cells/well in complete medium and cultured in CO_2-incubator for a day, creating conditions for cell adhesion to the bottom of the wells. On the day of the experiment the dispersions of micellar-encapsulated oxalates were prepared as specified above (S9 Section) using serum-free DMEM as a dispersion medium. Then the complete medium was removed from the wells of the plate and 0.2 ml/well of test compounds of different concentrations were added. Each dilution of each compound was tested on cells in 3 - 4 parallels, i.e. in 3 - 4 wells. The control wells were filled with 0.2 ml of medium without additives. Cells were incubated with the test substances for 1 - 1.5 hours in CO_2 incubator, then they were removed and cells were cultured for three days in complete medium (0.2 ml/well) without additives.

The cytotoxicity of the sample was evaluated c at the end of the experiment by the number of live cells in the experimental wells compared to the control using MTT-test. Cytotoxicity of tested compounds was evaluated by their concentration corresponding to 50% survival of cells (IC50).

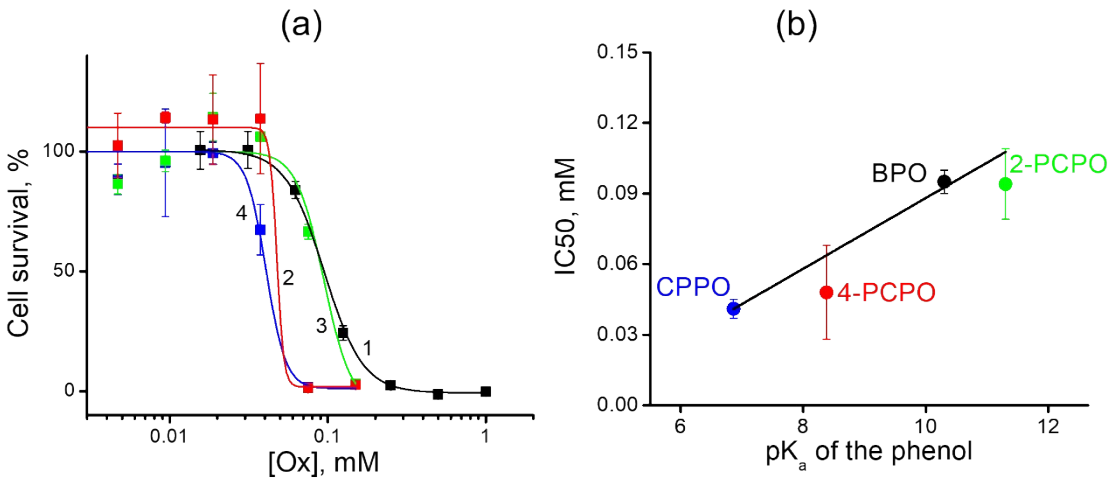

Fig. S19. (a) Survival of NCI-RES/ADR human ovarian adenocarcinoma cells in the presence of various concentrations of BPO (1), 4-PCPO (2), 2-PCPO (3), and CPPO (4). (b) Correlation of IC50 values with experimentally determined pKa of phenols.

References for ESI

1 G. Orosz, The role of diaryl oxalates in peroxioxalate chemiluminescence. Tetrahedron, 45, 3493-3506, 1989, https://doi.org/10.1016/S0040-4020(01)81028-0

2 A. F. Freeman, H. L. Haller (1938). The Preparation of Amyl Salicylates. J. Am. Chem. Soc., 60(9), 2274–2275. doi:10.1021/ja01276a502

3 D. Lee, V. R Erigala, M. Dasari, J. Yu, R. M Dickson, N. Murthy, Detection of hydrogen peroxide with chemiluminescent micelles. Int J Nanomedicine. 2008 Dec;3(4):471–476. PMID: 19337415; PMCID: PMC2636589.

4 H. Neuvonen, K. Neuvonen, Correlation analysis of carbonyl carbon 13C NMR chemical shifts, IR absorption frequencies and rate coefficients of nucleophilic acyl substitutions. A novel explanation for the substituent dependence of reactivity. J. Chem. Soc., Perkin Trans. 2, 1999, 1497–1502.

5 Souza, G. A., M. M. M. Peixoto, A. P. F. Santos and W. J. Baader (2016) General acid and base catalysis by phosphate in peroxyoxalate chemiluminescence. ChemistrySelect 1, 2307–2315

6 SDBS No.:1068 Spectral code:CDS-03-629 InChI=1S/C4H6O4/c1-7-3(5)4(6)8-2/h1-2H3, National Institute of Advanced Industrial Science and Technology (AIST), 1999-03-31

7 SDBS No.:2659 Spectral code:CDS-11-797. National Institute of Advanced Industrial

Science and Technology (AIST). 1999-03-31

8 A.G. Hadd and J.W. Birks Kinetics and Mechanism of the Nucleophilic Substitution Reaction of Imidazole with Bis(2,4,6-trichlorophenyl) Oxalate and Bis(2,4-dinitrophenyl) Oxalate. J. Org. Chem. 1996, 61, 2657-2663.

9 F.A. Augusto, F.H. Bartoloni, A.P.E. Pagano, W.J. Baader Mechanistic Study of the Peroxyoxalate System in Completely Aqueous Carbonate Buffer. Photochem. Photobiol. 2021, 97, 309–316.

10 Osbild S., Brault L., Battaglia E., Bagrel D. Resistance to cisplatin and adriamycin is associated with the inhibition of glutathione efflux in MCF-7-derived cells. Anticancer Res. 2006. 26. 5 A. 3595–3600.

11 European Collection of Authenticated Cell Cultures. Cell Line Profile MCF7. ECACC catalogue no. 86012803.